



HAL
open science

Calcium stable isotopes place Devonian conodonts as first level consumers

V. Balter, J.E. Martin, T. Tacail, G. Suan, Sabrina Renaud, Catherine Girard

► To cite this version:

V. Balter, J.E. Martin, T. Tacail, G. Suan, Sabrina Renaud, et al.. Calcium stable isotopes place Devonian conodonts as first level consumers. *Geochemical Perspectives Letters*, 2019, 10, pp.36-39. 10.7185/geochemlet.1912 . hal-02112869

HAL Id: hal-02112869

<https://hal.science/hal-02112869v1>

Submitted on 27 Apr 2019

HAL is a multi-disciplinary open access archive for the deposit and dissemination of scientific research documents, whether they are published or not. The documents may come from teaching and research institutions in France or abroad, or from public or private research centers.

L'archive ouverte pluridisciplinaire **HAL**, est destinée au dépôt et à la diffusion de documents scientifiques de niveau recherche, publiés ou non, émanant des établissements d'enseignement et de recherche français ou étrangers, des laboratoires publics ou privés.

Calcium stable isotopes place Devonian conodonts as first level consumers

V. Balter^{1*}, J.E. Martin¹, T. Tacail², G. Suan¹, S. Renaud³, C. Girard⁴



doi: 10.7185/geochemlet.1912

Abstract



Conodont animals are an extinct group of jawless vertebrates whose hard parts, also known as conodont elements, represent the earliest evidence of a mineralised skeleton in the vertebrate lineage. Conodont elements are interpreted as parts of a feeding apparatus, which together with the presence of eyes and microwear patterns, support the controversial hypothesis that conodont animals were macrophagous predators and/or scavengers. Here, we explore the trophic position of five conodont genera (*Palmatolepis*, *Polygnathus*, *Ancyrodella*, *Ancyrognathus* and *Icriodus*) from five contemporary Late Devonian sites distributed worldwide (France, Morocco, Vietnam and Australia) by means of calcium (Ca) stable isotope compositions. The seawater Ca isotope composition was calibrated using contemporary Late Devonian brachiopod isotopic values. By comparison with extant marine trophic chain composed of cartilaginous fish, conodont Ca isotope compositions are indicative of a zooplanktivore – primary piscivore niche, with

no genus-specific trophic pattern. The question of active predation or scavenging cannot be resolved definitively but our results strongly suggest that Late Devonian conodonts were first level consumers.

Received 17 September 2018 | Accepted 17 March 2019 | Published 26 April 2019

Introduction

Until the publication of the discovery of the first specimen of the conodont animal in 1983 with conodont elements *in situ* forming a feeding apparatus, the nature and function of the conodont elements was one of palaeontology's great mysteries (Briggs *et al.*, 1983). Since then, several other specimens have shown similar schemes for this feeding apparatus, in which the anterior elements form a structure allowing them to trap food that is further processed by the posterior elements (Purnell and Donoghue, 1997). Today, despite the advancement of synchrotron microtomography that allows reconstructing virtual movements of the elements forming the feeding apparatus (Goudemand *et al.*, 2011), the dietary behaviour of conodonts remains an open debate but recently Shirley *et al.* (2018) suggested a predatory or scavenger mode of life. Conodonts possessed sclerotic eye capsule and extrinsic eye musculature (Gabbott *et al.*, 1995; Purnell, 1995a), consistent with conodonts having pattern vision and an active predatory lifestyle. Lastly, microwear patterns were found on conodont elements, which constituted the first direct evidence that they functioned as teeth (Purnell, 1995b).

In the present work, which is a pilot study, we use for the first time calcium (Ca) stable isotopes to infer the feeding habit

of conodont animals. The first studies showing that trophic levels of animals, including fish, could be inferred from the Ca isotope compositions of their shell or inner skeleton lay back in the 2000's (Skulan *et al.*, 1997; Skulan and DePaolo, 1999; Clementz *et al.*, 2003; DePaolo, 2004). These results were recently confirmed on modern and fossil elasmobranchs (Martin *et al.*, 2015), a subclass of cartilaginous fish, including the sharks, rays and skates, and sawfish. Some authors have already measured the Ca isotope composition of conodonts but with the aim to reconstruct variations of the seawater composition (Hinojosa *et al.* 2012; Jost *et al.* 2014; Le Houedec *et al.* 2017). Here, the Late Devonian period, particularly the Frasnian-Famennian boundary (F/F), was chosen because it is accompanied by important variations in the shape of conodont elements, suggestive of changes in the feeding behaviour of several genera (Balter *et al.*, 2008; Girard and Renaud, 2008). The Material and Method sections are described in the Supplementary Information.

Results

All values presented in this work are expressed as $\delta^{44/42}\text{Ca}$ and defined as $\delta^{44/42}\text{Ca} = ((^{44}\text{Ca}/^{42}\text{Ca}_{\text{sample}}) / (^{44}\text{Ca}/^{42}\text{Ca}_{\text{SRM915a}}) - 1) * 1000$. All measured samples were plotted as $\delta^{43/42}\text{Ca}$ against

1. Laboratoire de Géologie de Lyon. UMR 5276 CNRS, ENS Lyon, Univ. Lyon1. 46, Allée d'Italie, 69342 Lyon Cedex 07, France
 2. Bristol Isotope Group, School of Earth Sciences, University of Bristol, Wills Memorial Building, Queen's Road, Bristol, BS8 1RJ, UK
 3. Laboratoire de Biométrie et Biologie Evolutive. UMR 5558 CNRS, Univ. Lyon1. Bâtiment Mendel. 43, bd du 11 novembre 1918, 69622 Villeurbanne Cedex, France
 4. Institut des Sciences de l'Evolution de Montpellier. UMR 5554 CNRS, Univ. Montpellier 2 Place Eugene Bataillon, 34095 Montpellier Cedex 05, France
- * Corresponding author (email: Vincent.Balter@ens-lyon.fr)



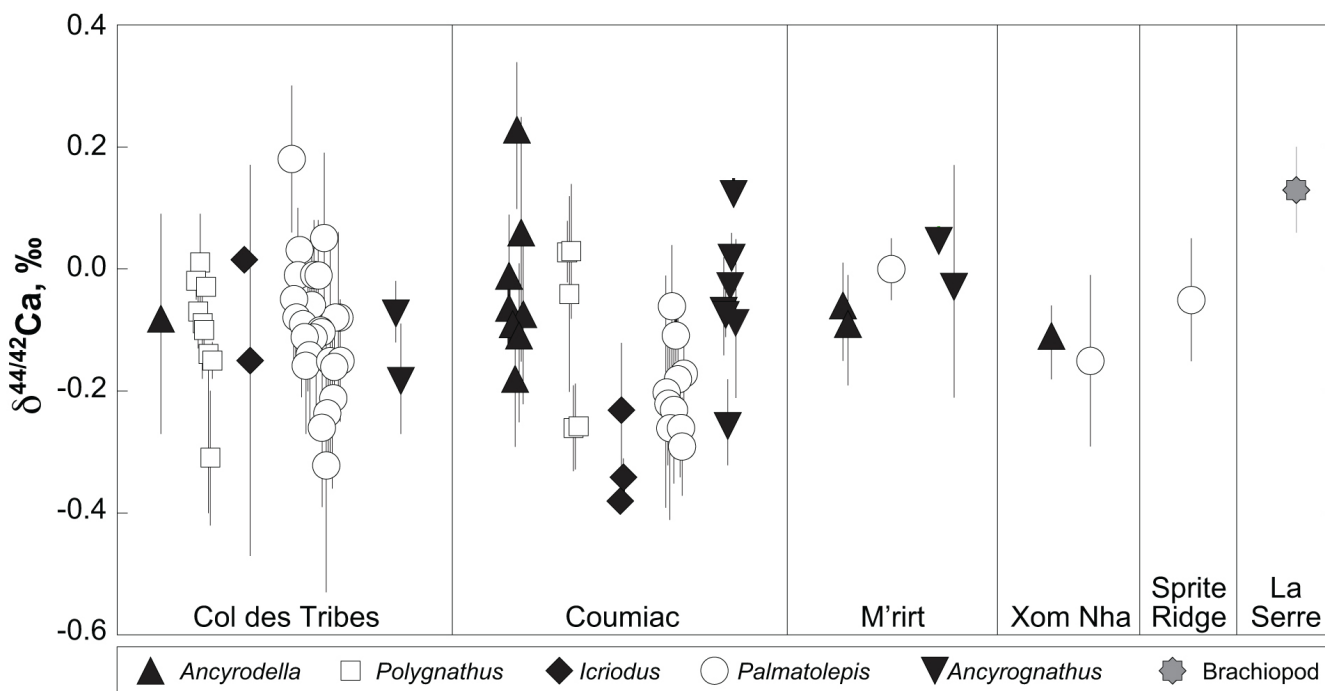


Figure 1 Ca isotope compositions of conodonts ($\delta^{44/42}\text{Ca}$) relative to SRM915a (‰) measured in the study.

$\delta^{44/42}\text{Ca}$ and fall on a line with a slope of 0.557 close to the theoretical 0.507 slope predicted by the exponential approximation of mass dependent fractionation (Tacail *et al.*, 2014; Fig. S-2). Quality control assessment is given in Table S-2, and Ca isotope values of conodonts measured in this study (Table S-3; Fig. 1) range from -0.38 ‰ to 0.22 ‰, with an average value of -0.10 ± 0.22 ‰ (± 2 s.d., $n = 80$). The average $\delta^{44/42}\text{Ca}$ value is -0.10 ± 0.20 ‰ (± 2 s.d., $n = 39$) at Col des Tribes, -0.12 ± 0.28 ‰ (± 2 s.d., $n = 39$) at Coumiac, -0.03 ± 0.12 ‰ (± 2 s.d., $n = 5$) at M'rt, -0.14 ± 0.04 ‰ (± 2 s.d., $n = 2$) at Xom Nha and -0.05 ‰ at Sprite Ridge (Table S-3). Comparison between conodonts at Coumiac and Col des Tribes, the two most abundant sites, reveals no significant difference of the $\delta^{44/42}\text{Ca}$ value (Student's *t*-test, $p = 0.373$). Comparisons between conodonts grouped by genus reveal no taxonomic difference (Table S-4). The brachiopod yielded a $\delta^{44/42}\text{Ca}$ value of 0.13 ‰ (Table S-1), which represents one of the highest values of the dataset.

Discussion

The present paper focuses on the trophic position of conodont animals based on their Ca isotope compositions, but these could have been affected by diagenetic processes. Discussion on the effects of diagenesis is developed in the Supplementary Information. We conclude, in the absence of any evidence of Ca isotope compositions being diagenetically reworked, that the measured $\delta^{44/42}\text{Ca}$ values of conodonts are biogenic.

The present paper focuses on the trophic position of conodont animals based on their Ca isotope composition, but accurate comparisons with modern analogues first necessitate calibrating the Ca isotopic values of the conodont elements relative to that of the contemporaneous seawater. Based on the existing Ca isotopic fractionation factor between modern brachiopods (br) *Terebratalia* and seawater (sw), $\alpha_{\text{br-sw}} = 0.99915$ (Gussone *et al.*, 2005), the $\delta^{44/42}\text{Ca}$ value of end-Devonian seawater ($\delta^{44/42}\text{Ca}_{\text{sw}}$) was estimated at 0.55 ‰, *i.e.* ~ 0.4 ‰ lower than that of modern oceans (Blättler *et al.* 2012). With an age estimated slightly younger than the Devonian-Carboniferous boundary of 360 Ma, this value falls in the range, but

in the lower limit, of the reconstructed Phanerozoic seawater Ca isotope composition of Farkaš *et al.* (2007; Fig. S-3). We can now calculate the Ca isotopic offset between seawater and conodonts, which is equal to 0.65 ± 0.25 ‰, (\pm s.d., $n = 80$). Conodonts are made up of hydroxylapatite (hap), which is more or less fluorinated, but it is the same mineral phase as that of elasmobranch teeth. This allows comparing the average Ca isotopic offset between Devonian seawater and conodonts with that of modern seawater and extant elasmobranch tooth enameloid (Martin *et al.* 2015), which is annotated $\Delta^{44/42}\text{Ca}_{\text{sw-hap}}$ (Fig. 2). Using a modern seawater $\delta^{44/42}\text{Ca}_{\text{sw}}$ value of 0.92 ‰, an offset of ~ 0.65 ‰ is observed nowadays between seawater and the zooplanktivore and primary piscivore group, which are characterised by average $\Delta^{44/42}\text{Ca}_{\text{sw-hap}}$ values of 0.56 ± 0.27 ‰ (± 2 s.d., $n = 5$) and 0.86 ± 0.08 ‰ (± 2 s.d., $n = 6$), respectively (Fig. 2). To fully encompass the $\delta^{44/42}\text{Ca}_{\text{sw}}$ variability at that time, which is well described by the study of Farkaš *et al.* (2007), we can also calculate the $\Delta^{44/42}\text{Ca}_{\text{sw-hap}}$ with the upper limit of the contemporaneous $\delta^{44/42}\text{Ca}_{\text{sw}}$ value, *i.e.* ~ 0.67 ‰. Even with this higher value, the calculated $\Delta^{44/42}\text{Ca}_{\text{sw-hap}}$ offset shows that conodonts are still in the the zooplanktivore - primary piscivore group (Fig. 2). The observation that conodonts fall as first level consumers is in accordance with the macrophagous hypothesis (*i.e.* feeding on relatively large particles of food), but is at odds with the view that conodont animals had a purely predatory lifestyle, which would have implied a $\delta^{44/42}\text{Ca}$ value of conodont elements around 1 ‰. Scavenging of fish cannot be ruled out, but must have involved small fish above all, otherwise the $\delta^{44/42}\text{Ca}$ values would have been those of predators.

Another argument in favour of a basal trophic position for conodonts, is that modern piscivore elasmobranchs exhibit a much tighter grouping of the $\delta^{44/42}\text{Ca}$ values than modern zooplanktivore elasmobranchs and conodonts (Figs. 1 and 2). The range of $\delta^{44/42}\text{Ca}$ values for a given trophic level of piscivore elasmobranchs never exceeds 0.1 ‰ while it is higher than 0.2 ‰ for modern zooplanktivore elasmobranchs and conodonts. No definitive explanation can be put forward from the state of the results, but a reasonable hypothesis could be that animals at the bottom of the trophic chain are more likely to sample local isotopic heterogeneities. This variability

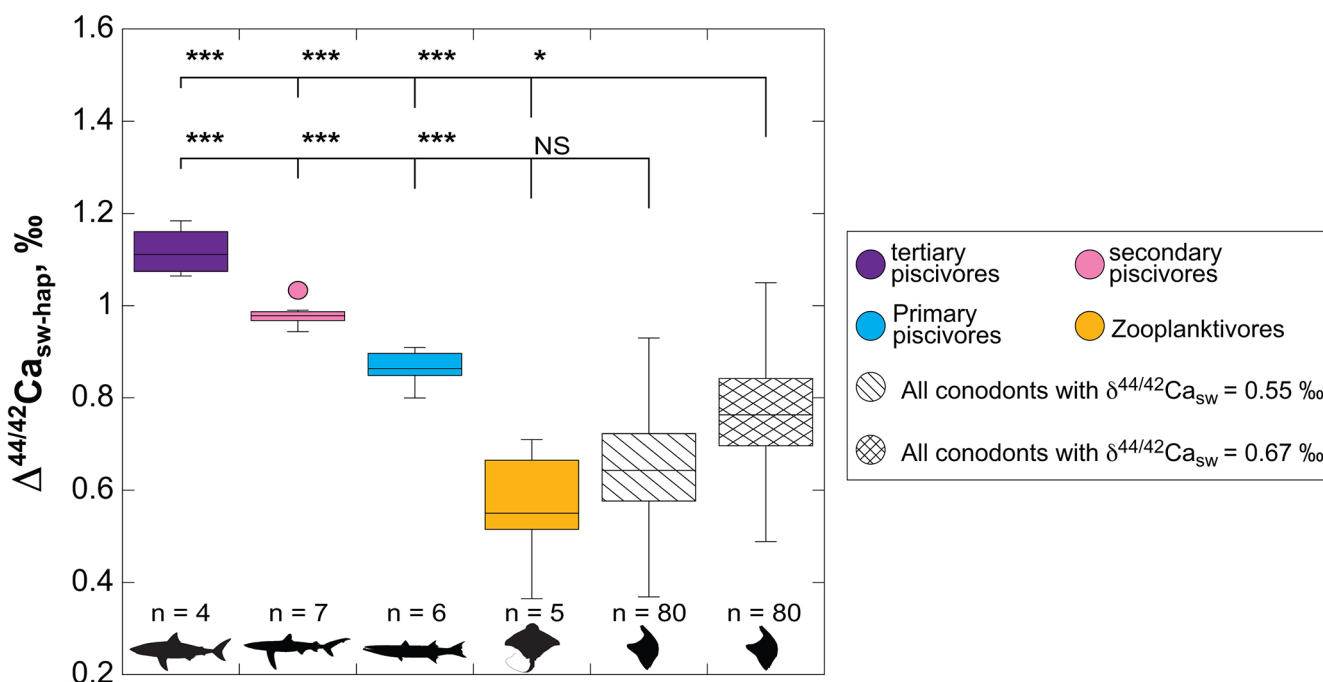


Figure 2 Ca isotopic offset between seawater and hap of modern elasmobranchs compared to that of conodonts ($\Delta^{44/42}\text{Ca}_{\text{sw-hap}}$) measured in the study. Modern elasmobranch data are from Martin *et al.* (2015). The $\Delta^{44/42}\text{Ca}_{\text{sw-hap}}$ offset is calculated with two $\delta^{44/42}\text{Ca}_{\text{sw}}$ values, 0.55 ‰ (diagonal lines) and 0.67 ‰ (diagonal cross hatch) corresponding to the range given by Farkaš *et al.* (2007; Fig. S-3). Boxplots delimit 5, 25, 50, 75 and 95 % percentiles. Depending on the $\delta^{44/42}\text{Ca}_{\text{sw}}$ value, statistics show that conodonts and zooplanktivores have similar $\delta^{44/42}\text{Ca}$ values. Under the null hypothesis that there is no difference in the distribution of two groups of $\delta^{44/42}\text{Ca}$ values, the p value of Student's *t*-tests provides the smallest level of significance at which null hypothesis would be rejected (NS, non-significant *p* value; **p* = 0.01–0.05; ***p* = 0.001–0.01; and ****p* < 0.001).

is subsequently contracted at higher trophic level probably thanks to a biopurification process such as in the case of the Sr/Ca and Ba/Ca ratios (Peek and Clementz, 2012).

The present results suggest that no significant difference in trophic level may have existed among conodonts, because genera exhibit indistinguishable $\delta^{44/42}\text{Ca}$ values (Table S-2). This overall similarity suggests that competition must have existed between some genera occupying similar trophic levels at the same time, *i.e.* between *Palmatolepis* and *Polygnathus* for instance. It is noteworthy that *Ancyrodella* is the only genus analysed in the study that disappeared at the F/F boundary, questioning the possibility that a distinct ecological trait would have triggered the extinction of this conodont genus.

Using a similar $\Delta^{44/42}\text{Ca}_{\text{sw-hap}}$ for conodont elements and modern elasmobranchs to retrieve the trophic position of conodont animals implies similar vital effects (*i.e.* isotope fractionation due to biological processes) in both groups. This approach is however probably simplistic. In fish, Ca is taken up along three pathways, (1) directly from the water *via* the gills, which contain a lot of ion-transporting cells or chloride cells (also known as ionocytes), but also through the intestine from (2) drinking water and (3) food (Flik and Verboost, 1993). No evidence for gills has ever been reported in preserved specimens of conodont animals (Aldridge and Purnell, 1996), which would suggest distinct $\Delta^{44/42}\text{Ca}_{\text{sw-hap}}$ values between conodont animals and elasmobranchs. Total intestinal absorption of calcium in marine fish represents around 30 % of the total calcium intake (Björnsson and Nilsson, 1985; Sundell and Björnsson, 1988). To our knowledge, relative proportions of drinking water and food in fish have never been determined, but the isotopic results of Martin *et al.* (2015) in elasmobranchs demonstrate that food must make a sizable proportion, otherwise no trophic effect would have been observed. Indeed, the most likely explanation to account for the depletion of Ca heavy isotopes up trophic chains, being marine or terrestrial, is that preys are wholly ingested along with their skeleton

which is depleted in heavy Ca isotopes. If the three types of Ca uptake described above are characterised by different isotope fractionation intensity, and their relative proportions vary between fish groups, this should in principle result in a different $\Delta^{44/42}\text{Ca}_{\text{sw-hap}}$ fractionation. Analysis of dietary relevant trace elements for marine organisms, such as Sr/Ca and Ba/Ca ratios (Balter and Lécuyer, 2004, 2010; Le Houedec *et al.*, 2013; Peek and Clementz, 2012) would corroborate the present results, but we question whether this would be feasible in light of the difference of vital effects discussed above, and of potential diagenetic effects. Further analysis of Ca isotopes in conodont assemblages will document the diversity of their ecological niches within Palaeozoic oceanic trophic chains.

Acknowledgements

We thank two anonymous reviewers for their insightful comments on an earlier version of the manuscript and R. Feist (Montpellier) who provided us with the brachiopod shell analysed in this work. This study was supported by the ANR project Ecodev (ANR-13-BSV7-0005). ISEM contribution 2019-071.

Editor: Ariel Anbar

Additional Information

Supplementary Information accompanies this letter at <http://www.geochemicalperspectivesletters.org/article1912>.



This work is distributed under the Creative Commons Attribution Non-Commercial No-Derivatives 4.0 License, which permits unrestricted distribution provided the original author and source

are credited. The material may not be adapted (remixed, transformed or built upon) or used for commercial purposes without written permission from the author. Additional information is available at <http://www.geochemicalperspectivesletters.org/copyright-and-permissions>.

Cite this letter as: Balter, V., Martin, J.E., Tacail, T., Suan, G., Renaud, S., Girard, C. (2019) Calcium stable isotopes place Devonian conodonts as first level consumers. *Geochem. Persp. Let.* 10, 36–39.

References

- ALDRIDGE, R.J., PURNELL, M.A. (1996) The conodont controversies. *Trends in Ecology and Evolution* 11, 463–468.
- BALTER V., LÉCUYER C. (2004) Determination of Sr and Ba partitioning coefficients between apatite and water from 5°C to 60°C: a new thermometer for aquatic environments. *Geochimica et Cosmochimica Acta* 68, 423–432.
- BALTER V., LÉCUYER C. (2010) Determination of Sr and Ba partition coefficients between apatite from fish (*Sparus aurata*) and seawater: the influence of temperature. *Geochimica et Cosmochimica Acta* 74, 3449–3458.
- BALTER V., RENAUD S., GIRARD C., JOACHIMSKI M. (2008) The record of climate-driven morphological changes in 376 Ma old Devonian fossils. *Geology* 36, 907–910.
- BLÄTTLER, C.L., HENDERSON, G.M., JENKINS, H.C. (2012) Explaining the Phanerozoic Ca isotope history of seawater. *Geology* 40, 843–846.
- BJÖRNSSON, B.T., NILSSON, S. (1985) Renal and extrarenal excretion of calcium in the marine teleost, *Gadus morhua*. *American Journal of Physiology* 248, 18–22.
- BRIGGS, D.E.G., CLARKSON, E.N.K., ALDRIDGE, R.J. (1983) The conodont animal. *Lethaia* 16, 1–14.
- CLEMENTZ, M. T., HOLDEN, P., KOCH, P.L. (2003) Are Calcium isotopes a reliable monitor of trophic level in marine settings? *International Journal of Osteoarchaeology* 13, 29–36.
- DEPAOLO, D.J., (2004) Calcium Isotopic Variations Produced by Biological, Kinetic, Radiogenic and Nucleosynthetic Processes. *Reviews in Mineralogy and Geochemistry* 55, 255–288.
- FARKAŠ, J., BÖHM, F., WALLMANN, K., BLENKINSOP, J., EISENHAEUER, A., VAN GELDERN, R., MUNNECKE, A., VOIGT, S., VEIZER, J. (2007) Calcium isotope record of Phanerozoic oceans: implications for chemical evolution of seawater and its causative mechanisms. *Geochimica et Cosmochimica Acta* 71, 5117–5134.
- FLIK, G., VERBOST, P.M. (1993) Calcium transport in fish gills and intestine. *Journal of Experimental Biology* 184, 17–29.
- GABBOTT, S.E., ALDRIDGE, R.J., THERON, J.N. (1995) A giant conodont with preserved muscle tissue from the Upper Ordovician of south Africa. *Nature* 374, 800–803.
- GIRARD, C., RENAUD, S. (2008) Disentangling allometry and response to Kellwasser anoxic events in the Late Devonian conodont genus *Ancyrodella*. *Lethaia* 41, 383–394.
- GOUEMAND, N., ORCHARD, M.J., URDY, S., BUCHER, H., TAFFOREAU, P. (2011) Synchrotron-aided reconstruction of the conodont feeding apparatus and implications for the mouth of the first vertebrates. *Proceedings of the National Academy of Sciences USA* 108, 8720–8724.
- GUSSONE, N., BÖHM, F., EISENHAEUER, A., DIETZEL, M., HEUSER, A., TEICHERT, B.M.A., REITNER, J., WÖRHEIDE, G., DULLO, W.C. (2005) Calcium isotope fractionation in calcite and aragonite. *Geochimica et Cosmochimica Acta* 69, 4485–4494.
- HINOJOSA, J.L., BROWN, S.T., CHEN, J., DEPAOLO, D.J., PAYTAN, A., SHEN, S.-Z., PAYNE, J.L. (2012) Evidence for end-Permian ocean acidification from calcium isotopes in biogenic apatite. *Geology* 40, 743–746.
- JOST, A., MUNDIL, R., HE, B., BROWN, S.T., ALTINER, D., SUN, Y., DEPAOLO, D.J., PAYNE, J.L. (2014) Constraining the cause of the end-Guadalupian extinction with coupled records of carbon and calcium isotopes. *Earth and Planetary Science Letters* 396, 201–212.
- LE HOUËDEC, S., GIRARD, C., BALTER, V. (2013) Conodont Sr/Ca and $\delta^{18}\text{O}$ record seawater changes at the Frasnian-Famennian boundary. *Palaeogeography, Palaeoclimatology, Palaeoecology* 376, 114–121.
- LE HOUËDEC, S., MCCULLOCH, M., TROTTER, J., RANKENBURG, K. (2017) Conodont apatite $\delta^{88/86}\text{Sr}$ and $\delta^{44/40}\text{Ca}$ compositions and implications for the evolution of Palaeozoic to early Mesozoic seawater. *Chemical Geology* 453, 55–65.
- MARTIN, J.E., TACAİL, T., ADNET, S., GIRARD, C., BALTER, V. (2015) Calcium isotopes reveal the trophic position of extant and fossil elasmobranchs. *Chemical Geology* 415, 118–125.
- PEEK, S., CLEMENTZ, M.T. (2012) Sr/Ca and Ba/Ca variations in environmental and biological sources: A survey of marine and terrestrial systems. *Geochimica et Cosmochimica Acta* 95, 36–52.
- PURNELL, M.A. (1995a) Large eyes and vision in conodonts. *Lethaia* 28, 187–188.
- PURNELL, M.A. (1995b) Microwear on conodont elements and macrophagy in the first vertebrates. *Nature* 374, 798–800.
- PURNELL, M.A., DONOGHUE, P.C.J. (1997) Architecture and functional morphology of the skeletal apparatus of ozarkonid conodonts. *Philosophical Transactions of the Royal Society* 352, 1545–1564.
- SHIRLEY, B., GROHGANZ, M., BESTMANN, M., JAROCZOWSKA, E. (2018) Wear, tear and systematic repair: testing models of growth dynamics in conodonts with high-resolution imaging. *Proceedings of the Royal Society B: Biological Sciences* 285, doi: 10.1098/rspb.2018.1614.
- SKULAN, J., DEPAOLO, D.J. (1999) Calcium isotope fractionation between soft and mineralised tissues as a monitor of calcium use in vertebrates. *Proceedings of the National Academy of Sciences USA* 96, 13709–13713.
- SKULAN, J., DEPAOLO, D.J., OWENS, T.L. (1997) Biological control of calcium isotopic abundances in the global calcium cycle. *Geochimica et Cosmochimica Acta* 61, 2505–2510.
- SUNDELL, K., BJÖRNSSON, B.T. (1988) Kinetics of calcium fluxes across the intestinal mucosa of the marine teleost, *Gadus morhua*, measured using an in vitro perfusion method. *Journal of Experimental Biology* 140, 170–186.
- TACAİL T., ALBALAT E., TÉLOUK P., BALTER V. (2014) A simplified protocol for the measurement of Ca isotopes in biological samples. *Journal of Analytical Atomic Spectrometry* 29, 529–535.



■ Calcium stable isotopes place Devonian conodonts as first level consumers

V. Balter, J.E. Martin, T. Tacail, G. Suan, S. Renaud, C. Girard

■ Supplementary Information

The Supplementary Information includes:

- Supplementary Material
- Supplementary Method
- Supplementary Discussion
- Tables S-1 to S-5
- Figures S-1 to S-3
- Supplementary Information References

Supplementary Material

Conodont elements were collected from Frasnian-Famennian levels of five different localities (Figure S-1): 1) a Famennian succession at the Col des Tribes (France), a newly described outcrop in the Montagne Noire, which exposes a continuous record of the Famennian Stage (Girard *et al.* 2014); 2) the stratotype area of the F/F boundary, the Coumiac Lower Quarry, located close to the Col des Tribes (Girard and Feist 1997); 3) M'ritt (Central Meseta, Morocco), which shows a similar environmental context to Coumiac, where deposits are a succession of well-oxygenated beds (Lazreq 1999). Conodonts are sampled from the *Pa. linguiformis* Zone (M9, level just before the Upper Kellwasser event) (Girard *et al.* 2005); 4) the Xom Nha section (Central Vietnam), which is characterised by a continuous carbonate sequence dated from latest Frasnian to Famennian (here the conodonts are from the *Pa. linguiformis* Zone XN52, Phuong 1998); 5) Sprite Ridge (Canning Basin, Australia), which is part of an elongated Famennian limestone (Feist and Becker 1997). The sample analysed here is of the *Early rhomboidea* Zone. In addition, a brachiopod sample was collected from the La Serre section in the *Bispathodus ultimus* zone corresponding to the CT69 level at Col des Tribes. All correlations are based on conodont biostratigraphy (Flajs and Feist 1988; Girard and Feist 1997; Girard *et al.* 2010, 2014), and absolute ages are given in Figure S-1 according to Becker *et al.* (2012). All the samples came from stratigraphic levels around the F/F boundary which is dated of ~ 372 Ma. Calcium isotopes were measured in a total of 80 conodont samples, which are distributed as follows: *Palmatolepis*, n = 38; *Ancyrodella*, n = 12; *Ancyrognathus*, n = 11; *Icriodus*, n = 5; *Polygnathus*, n = 14. For each studied stratigraphic level and for a given genus, between five and twenty conodont elements (depending on their size and the richness of the stratigraphic layer) were selected and completely dissolved in 1 ml ultrapure concentrated HNO₃ overnight. The brachiopod shell was sampled following the protocol of Brazier *et al.* (2015) and dissolved as for the conodonts.



Supplementary Methods

The details of the purification processes and analytical techniques are given in Tacail *et al.* (2014) but are summarised here. Samples were digested on hotplate using 2 ml concentrated distilled HNO₃. Vials were heated at 120°C during 2 h and regularly degassed. A volume of 2 ml Suprapur 30 % H₂O₂ was added on cooled samples and vials were sealed, regularly degassed at ambient temperature. Finally, vials were sealed and heated on hotplate at 100°C during 2 h and evaporated to dryness. The use of MC-ICPMS requires efficient separation of Ca from samples because of isobaric interferences. Strontium, potassium and to a lesser extent magnesium from samples have to be eliminated to avoid any bias in the measurement of ⁴²Ca⁺ (interfering with ⁸⁴Sr²⁺, ⁴¹K^{1H+} and ²⁵Mg¹⁶O⁺), ⁴³Ca⁺ (⁸⁶Sr²⁺) and ⁴⁴Ca⁺ (⁸⁸Sr²⁺, ²⁶Mg¹⁸O⁺). The elimination of the remaining matrix components is also required to avoid any bias due to matrix effects. The exact elution procedure is shown in Table S-1.

The first elution aims at discarding K and the majority of matrix elements. Once taken up in 1N HCl, samples were processed on 0.76 cm internal diameter Teflon chromatography columns, filled with 2 ml of Biorad AG50W-X12 cationic resin, 200-400 mesh. The AG50W-X12 columns were reused maximum 5 times, in order to avoid any aging of resin. Strontium was finally eliminated by processing samples on 0.7 ml Eichrom Sr-specific resin, packed in 2 ml Eichrom columns, following a classical Sr elimination protocol (Table S-1). Blank levels never exceed 100 ng, which would represent a contribution of 1/30 of a typical signal. The Sr/Ca ratio, measured as the ⁸⁷Sr²⁺/⁴⁴Ca⁺ ratio is always below 10⁻⁵. Quality control of the Ca chemical purification is controlled in each session by including a blank and one or two standards which are matrix-matched with the samples (SRM915b "Calcium Carbonate" and SRM1486 "Bone Meal"). Data for the standards are reported in Table S-2. Based on replicates of two standards, the external reproducibility has been estimated at ±0.066 ‰ (2 SD, n = 130) for SRM1486 and ±0.048 ‰ (2SD, n=17) for SRM915b in the context of the present study. Since 2014, the overall reproducibility of SRM1486 is ±0.006 (2 SE, n = 404) with a mean $\delta^{44/42}\text{Ca}$ value of -1.024 ‰.

The Ca isotopic compositions were measured using a Neptune plus MC-ICPMS (Thermo Scientific, Bremen, Germany). Standard and sample solutions were prepared to reach a 3 mg.l⁻¹ concentration in 0.05N HNO₃ medium. Calcium solution was introduced as a dry aerosol with a Cetac Aridus II desolvating system allowing reduction of hydride and oxide formation. The Aridus desolvating system was used with Ar sweep gas flow and an additional N₂ gas flow. Aerosols were introduced in a 1200 W plasma with uptake rate of 100 to 150 $\mu\text{L}\cdot\text{min}^{-1}$. The optimised MC-ICPMS instrument operating parameters were : cool gas (15 L.min⁻¹), auxiliary gas (0.7-0.8 L.min⁻¹) and sample gas (1-1.2 L.min⁻¹).

Faraday cups were set to measure ⁴²Ca⁺ signal on L4 cup, ⁴³Ca⁺ on L2 and ⁴⁴Ca⁺ on central cup. The use of these three isotopes is sufficient for mass-dependent stable isotopes composition measurements in biological materials. The L1 cup was used to monitor the ⁸⁷Sr²⁺ corresponding to m/z = 43.5. The 42 and 44 ion beams signals were measured with a 10¹¹ Ω resistance on faraday cup and 43 signal was measured with 10¹² Ω resistance, because of the low abundance of ⁴³Ca (0.135 % of total Ca). Calcium concentrations were adjusted to be within 10 % of the fixed 3 mg.l⁻¹ concentration. Medium mass resolution was sufficient to resolve polyatomic interferences: including ⁴⁰Ar¹H₂⁺, ¹²C¹⁶O₂⁺ and ¹⁴N₃⁺.

Each analysis consisted of 40 measurements of 4.2 s integrations on m/z ratios 42, 43, 44 and 43.5. Even if Sr levels were very low due to the specific separation on the Sr-Spec resin, we corrected the double charge interferences of Sr on Ca (⁸⁸Sr²⁺ on ⁴⁴Ca⁺, ⁸⁶Sr²⁺ on ⁴³Ca⁺, ⁸⁴Sr²⁺ on ⁴²Ca⁺) using the 43.5 signal corresponding to ⁸⁷Sr²⁺. The correction includes the instrumental mass bias on Sr isotopes, which was monitored using the NBS 987 standard. Corrected and uncorrected ratios were calculated for each measurement and averaged after exclusion of values higher than 1SD from average. Instrumental mass bias was corrected by standard-sample-standard bracketing. A Specpure Calcium plasma standard solution (Alfa Aesar), noted ICP-Lyon, was used as reference and bracketing in-house standard. ICP-Lyon required purification because of the presence of Sr traces responsible for significant interferences on the three measured isotopes.

Supplementary Discussion

Sedimentological analyses (Girard *et al.* 2014) at the Col des Tribes and geochemical analyses on bulk sediment ($\delta^{13}\text{C}$ and $\delta^{18}\text{O}$) at the Coumiac Quarry (Joachimski and Buggisch 1993) do not argue for any substantial post-depositional modifications. Regarding more specifically the Ca isotope composition of fossils, its use to unravel paleobiological features is in its infancy and data are still lacking to highlight potential methods to detect diagenesis of the original isotopic composition. Calcium is the major element of endogenous mineralised tissues, bone, dentine and enamel, which are made up of hydroxylapatite, and exogenous mineralised tissues, which are made up of calcite or aragonite. In both cases, Ca represents about 40 % weight of the mineral fraction, rendering Ca hardly prone to diagenesis because diagenetic fluids are incommensurably less Ca concentrated (Martin *et al.*, 2017). For instance, this led recently Pruss *et al.* (2018) to show that 600 Myr old Ediacaran shell-forming organisms had still preserved a Ca isotope signature typical of aragonite. Here, we did not measure the concentration of trace elements that specifically incorporate



hap during diagenetic processes, such as rare Earth elements (REE), due to sample size limitation. However, REE concentrations have been previously measured in conodonts at Coumiac along with the strontium/calcium ratio (Sr/Ca) and the oxygen isotope composition of phosphates ($\delta^{18}\text{O}$, Le Houedec *et al.*, 2014). From eight common layers where all the geochemical proxies have been measured, we show that, unless the strong correlation between La/Sm and La/Yb, indicative of substitution mechanisms in the context of 'extensive' or 'late' diagenesis (Reynard and Balter, 2014), no proxy is significantly correlated to any other (Table S-5).

Supplementary Tables

Table S-1 Chart of the purification processes.

1. Matrix elimination		
AG50W-X12 resin (200-400 mesh) ~ 2mL		
Step	Eluent	Vol. (mL)
Condition	1N HCl	10
Load	1N HCl	2+1
Elution (matrix)	1N HCl	55
Ca elution (Ca,Sr,Fe)	6N HCl	10
2. Sr elimination		
Sr-Specific resin (Eichrom) ~ 0.7mL		
Step	Eluent	Vol. (mL)
Condition	3N HNO ₃	5
Load	3N HNO ₃	0.5+0.5
Elution (Ca)	3N HNO₃	6
Remaining on resin: Sr		



Table S-2 Ca isotope compositions of SRM1486 and SRM915b measured in the study relative to ICP-Lyon.

Standard		n	$\delta^{44}/^{42}$ amu	2 SD	reference
SRM1486	session #				
	1	38	-0.52	0.02	
	2	29	-0.53	0.14	
	3	30	-0.50	0.07	
	4	7	-0.52	0.05	
	5	21	-0.48	0.08	
	6	5	-0.51	0.04	
	literature				
		25	-0.52	0.06	Martin <i>et al.</i> (2015)
		17	-0.48	0.07	Tacail <i>et al.</i> (2014)
		142	-0.51	0.07	Heuser and Eisenhauer (2008)*
	2	-0.50	0.07	Heuser <i>et al.</i> (2011)*	
SRM915b	session #				
	1	3	-0.11	0.03	
	2	3	-0.06	0.02	
	3	3	-0.06	0.09	
	4	2	-0.06	0.05	
	5	6	-0.10	0.05	
	literature				
		13	-0.08	0.06	Martin <i>et al.</i> (2015)
	11	-0.06	0.04	Tacail <i>et al.</i> (2014)	
	56	-0.08	0.01	Heuser and Eisenhauer (2008)*	

* TIMS analysis



Table S-3 Ca isotope compositions measured in the study relative to ICP-Lyon and SRM915a standards. Conversion between ICP-Lyon and SRM915a standards is given by the relationship: $\delta^{44/42}\text{Ca}_{\text{ICP-Lyon}} = \delta^{44/42}\text{Ca}_{\text{SRM915a}} - 0.52$ (Martin et al. 2015). Error of the $\delta^{44/42}\text{Ca}_{\text{SRM915a}}$ value is obtained by adding 0.08 ‰ on the error relative to ICP Lyon.

locality	ID	taxon	shape	n	$\delta^{44/42}\text{Ca}$	2 SD	$\delta^{43/42}\text{Ca}$	2 SD	$\delta^{44/42}\text{Ca}$
					vs. ICP Lyon		vs. ICP Lyon		vs. SRM915a
Col des Tribes	CT22An	<i>Ancyrodella</i>		2	-0.61	0.18	-0.32	0.08	-0.09
	CT22Ag	<i>Ancyrognathus</i>		2	-0.59	0.05	-0.28	0.01	-0.07
	CT23Ag	<i>Ancyrognathus</i>		3	-0.70	0.09	-0.35	0.01	-0.18
	CT22 (IC1)	<i>Icriodus</i>		2	-0.50	0.01	-0.19	0.03	0.02
	CT22 (IC2)	<i>Icriodus</i>		2	-0.67	0.32	-0.28	0.10	-0.15
	CT59-7	<i>Palmatolepis</i>		2	-0.34	0.12	-0.21	0.00	0.18
	CT37	<i>Palmatolepis</i>		2	-0.57	0.10	-0.27	0.07	-0.05
	CT35Pa	<i>Palmatolepis</i>		2	-0.60	0.08	-0.31	0.14	-0.08
	CT33	<i>Palmatolepis</i>		2	-0.53	0.11	-0.28	0.13	-0.01
	CT30Pa	<i>Palmatolepis</i>		2	-0.49	0.01	-0.29	0.02	0.03
	CT23Pa	<i>Palmatolepis</i>	Broad	6	-0.61	0.12	-0.30	0.12	-0.09
	CT39Pa	<i>Palmatolepis</i>	Broad	2	-0.63	0.07	-0.34	0.00	-0.11
	CT46Pa	<i>Palmatolepis</i>	Broad	6	-0.68	0.11	-0.35	0.08	-0.16
	CT51Pa1	<i>Palmatolepis</i>	Slender	5	-0.63	0.09	-0.33	0.15	-0.11
	CT51Pa2	<i>Palmatolepis</i>	Broad	5	-0.66	0.12	-0.34	0.06	-0.14
	CT54-2Pa	<i>Palmatolepis</i>	Broad	6	-0.58	0.12	-0.28	0.11	-0.06
	CT62Pa_1	<i>Palmatolepis</i>	Slender	4	-0.53	0.09	-0.26	0.05	-0.01
	CT62Pa_2	<i>Palmatolepis</i>	Broad	6	-0.63	0.12	-0.32	0.14	-0.11
	CT69GPa	<i>Palmatolepis</i>	Broad	8	-0.53	0.09	-0.28	0.08	-0.01
	CT56Pa	<i>Palmatolepis</i>	Broad	3	-0.62	0.01	-0.36	0.07	-0.10
	CT33FRPa	<i>Palmatolepis</i>	Broad	3	-0.78	0.13	-0.39	0.14	-0.26
	CT70-2_Pa	<i>Palmatolepis</i>	Broad	3	-0.47	0.14	-0.25	0.07	0.05
	CT35Pa0	<i>Palmatolepis</i>	Broad	3	-0.84	0.21	-0.48	0.13	-0.32
	CT22Pa	<i>Palmatolepis</i>	Broad	3	-0.76	0.10	-0.39	0.09	-0.24
	CT22 (Pa1)	<i>Palmatolepis</i>	Broad	2	-0.67	0.18	-0.40	0.09	-0.15
	CT22 (Pa2)	<i>Palmatolepis</i>	Broad	2	-0.73	0.15	-0.43	0.01	-0.21
	CT66Pa	<i>Palmatolepis</i>	Broad	2	-0.68	0.07	-0.36	0.03	-0.16
	CT66 (Pa5)	<i>Palmatolepis</i>	Broad	2	-0.60	0.02	-0.36	0.00	-0.08
	CT66 (Pa6)	<i>Palmatolepis</i>	Broad	2	-0.60	0.14	-0.34	0.04	-0.08
	CT66 (Pa7)	<i>Palmatolepis</i>	Broad	2	-0.67	0.10	-0.42	0.10	-0.15
	CT30Po	<i>Polygnathus</i>		3	-0.54	0.03	-0.29	0.06	-0.02
	CT46Po	<i>Polygnathus</i>		3	-0.59	0.06	-0.30	0.03	-0.07
	CT69GPa	<i>Polygnathus</i>		4	-0.51	0.08	-0.26	0.10	0.01
	CT39Po	<i>Polygnathus</i>		7	-0.61	0.09	-0.33	0.10	-0.09
	CT22Po	<i>Polygnathus</i>		2	-0.62	0.03	-0.29	0.05	-0.10
	CT51Po	<i>Polygnathus</i>		4	-0.55	0.00	-0.28	0.07	-0.03
	CT22 (Po1)	<i>Polygnathus</i>		2	-0.66	0.26	-0.25	0.20	-0.14
	CT22 (Po2)	<i>Polygnathus</i>		2	-0.83	0.11	-0.45	0.01	-0.31
	CT22 (Po3)	<i>Polygnathus</i>		2	-0.67	0.03	-0.31	0.07	-0.15



Coumiac	CUQ31cAn	<i>Ancyrodella</i>	2	-0.54	0.11	-0.29	0.02	-0.02	
	CLQ25aAn	<i>Ancyrodella</i>	2	-0.59	0.01	-0.25	0.07	-0.07	
	CUQ28cAn	<i>Ancyrodella</i>	2	-0.62	0.01	-0.32	0.02	-0.10	
	CLQ25bAn	<i>Ancyrodella</i>	3	-0.71	0.10	-0.37	0.06	-0.19	
	CLQ23An	<i>Ancyrodella</i>	3	-0.30	0.12	-0.16	0.15	0.22	
	CLQ24An	<i>Ancyrodella</i>	3	-0.64	0.13	-0.32	0.02	-0.12	
	CLQ25aAn	<i>Ancyrodella</i>	2	-0.47	0.20	-0.32	0.12	0.05	
	CLQ25bAn	<i>Ancyrodella</i>	3	-0.60	0.14	-0.31	0.19	-0.08	
	CLQ25aAg	<i>Ancyrognathus</i>	3	-0.58	0.08	-0.28	0.03	-0.06	
	CLQ23bAg	<i>Ancyrognathus</i>	2	-0.59	0.04	-0.30	0.02	-0.07	
	CLQ25bAg	<i>Ancyrognathus</i>	2	-0.77	0.07	-0.40	0.11	-0.25	
	CUQ31cAg	<i>Ancyrognathus</i>	1	-0.54		-0.29		-0.02	
	CUQ28cAg	<i>Ancyrognathus</i>	2	-0.49	0.03	-0.24	0.03	0.03	
	CLQ23Ag	<i>Ancyrognathus</i>	3	-0.39	0.02	-0.14	0.14	0.13	
	CLQ24Ag	<i>Ancyrognathus</i>	4	-0.60	0.13	-0.33	0.12	-0.08	
	CLQ28Ic	<i>Icriodus</i>	2	-0.90	0.01	-0.50	0.03	-0.38	
	CLQ29aIc	<i>Icriodus</i>	2	-0.75	0.11	-0.39	0.01	-0.23	
	CLQ33Ic	<i>Icriodus</i>	2	-0.86	0.03	-0.48	0.06	-0.34	
	CLQ23Pa	<i>Palmatolepis</i>	3	-0.72	0.19	-0.38	0.14	-0.20	
	CLQ24Pa	<i>Palmatolepis</i>	3	-0.74	0.10	-0.39	0.10	-0.22	
	CLQ25aPa	<i>Palmatolepis</i>	3	-0.78	0.15	-0.41	0.11	-0.26	
	CLQ25bPa	<i>Palmatolepis</i>	6	-0.58	0.10	-0.31	0.10	-0.06	
	CLQ26aPa	<i>Palmatolepis</i>	3	-0.75	0.12	-0.38	0.08	-0.23	
	CLQ26bPa	<i>Palmatolepis</i>	2	-0.63	0.04	-0.33	0.10	-0.11	
	CLQ27Pa	<i>Palmatolepis</i>	3	-0.70	0.12	-0.36	0.13	-0.18	
	CLQ28Pa	<i>Palmatolepis</i>	3	-0.78	0.08	-0.39	0.11	-0.26	
	CLQ29aPa	<i>Palmatolepis</i>	3	-0.81	0.08	-0.43	0.01	-0.29	
	CLQ33Pa	<i>Palmatolepis</i>	2	-0.69	0.06	-0.40	0.07	-0.17	
	CLQ25aPo	<i>Polygnathus</i>	3	-0.49	0.05	-0.25	0.02	0.03	
	CLQ25bPo	<i>Polygnathus</i>	3	-0.56	0.16	-0.29	0.07	-0.04	
	CLQ29aPo	<i>Polygnathus</i>	3	-0.49	0.11	-0.22	0.08	0.03	
	CLQ26bPo	<i>Polygnathus</i>	3	-0.78	0.07	-0.43	0.09	-0.26	
	CLQ28Po	<i>Polygnathus</i>	2	-0.78	0.07	-0.39	0.08	-0.26	
	M'ritt	M9-1An	<i>Ancyrodella</i>	2	-0.62	0.09	-0.32	0.01	-0.10
		M9-2An	<i>Ancyrodella</i>	2	-0.59	0.08	-0.29	0.04	-0.07
		M9-1Ag	<i>Ancyrognathus</i>	2	-0.47	0.02	-0.21	0.02	0.05
		M9-2Ag	<i>Ancyrognathus</i>	2	-0.54	0.19	-0.29	0.06	-0.02
	Xom Nha	M9Pa	<i>Palmatolepis</i>	2	-0.52	0.05	-0.25	0.05	0.00
		XNAn	<i>Ancyrodella</i>	3	-0.64	0.06	-0.33	0.03	-0.12
	Sprite Ridge	XNPa	<i>Palmatolepis</i>	2	-0.67	0.14	-0.34	0.09	-0.15
SR1		<i>Palmatolepis</i>	2	-0.57	0.10	-0.33	0.08	-0.05	
La Serre	LSbrach	brachiopod	3	-0.39	0.07	-0.20	0.03	0.13	



Table S-4 Statistical results (p -value) of Student's t -tests between conodont genera. Under the null hypothesis that there is no difference in the distribution of two groups of $\delta^{44/42}\text{Ca}$ values, the p -value provides the smallest level of significance at which null hypothesis would be rejected. (NS, non significant p value; * p = 0.01–0.05; ** p = 0.001–0.01; and *** p < 0.001).

	<i>Ancyrodella</i>	<i>Ancyrognathus</i>	<i>Icriodus</i>	<i>Palmatolepis</i>	<i>Polygnathus</i>
<i>Ancyrodella</i>		NS 0.849	NS 0.092	NS 0.092	NS 0.327
<i>Ancyrognathus</i>			NS 0.080	NS 0.068	NS 0.253
<i>Icriodus</i>				NS 0.250	NS 0.190
<i>Palmatolepis</i>					NS 0.586
<i>Polygnathus</i>					

Table S-5 Statistical results (correlation coefficient and associated p -value) of Student's t -tests between geochemical proxies used in the study (NS, non significant p value; * p = 0.01–0.05; ** p = 0.001–0.01; and *** p < 0.001).

	$\delta^{44/42}\text{Ca}$	$\delta^{18}\text{O}$	Sr/Ca	La/Yb	La/Sm
$\delta^{44/42}\text{Ca}$		-0.676, NS 0.066	0.730, NS 0.062	0.518, NS 0.233	0.483, NS 0.273
$\delta^{18}\text{O}$			-0.578, NS 0.174	0.048, NS 0.918	0.139, NS 0.767
Sr/Ca				0.139, NS 0.767	0.152, NS 0.745
La/Yb					0.958, *** <10 ⁻⁴
La/Sm					



Supplementary Figures

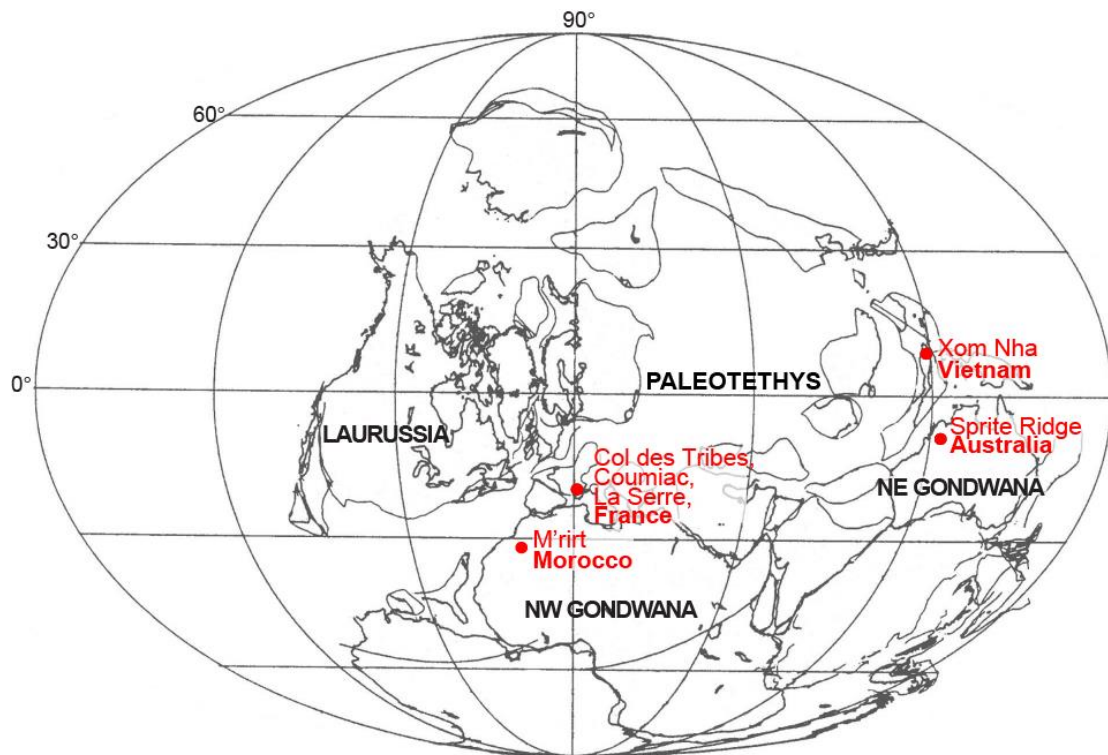


Figure S-1 Localisation of the different sites discussed in the text. Absolute ages are for Col des Tribes, -374 to -360 My; Coumiac, -374 to -371 My; M'ritt and Xom Nha: around -373 My; Sprite Ridge, around 367.5 My. La Serre, -360 My. Ages are from Becker et al. (2012). Conodonts are distributed as following: Col des Tribes, n = 39 (*Palmatolepis*, n=25; *Ancyrodella*, n=1; *Ancyrognathus*, n=2; *Icriodus* n=2; *Polygnathus*, n=9); Coumiac, n = 32 (*Palmatolepis*, n=10; *Ancyrodella*, n=8; *Ancyrognathus*, n=7; *Icriodus* n=2; *Polygnathus*, n=5); M'ritt, n = 5 (*Ancyrodella*, n=2; *Ancyrognathus*, n=2; *Palmatolepis*, n=1); Xom Nha, n = 2 (*Ancyrodella*, n=1; *Palmatolepis*, n=1); Sprite Ridge, n = 1 (*Palmatolepis*).

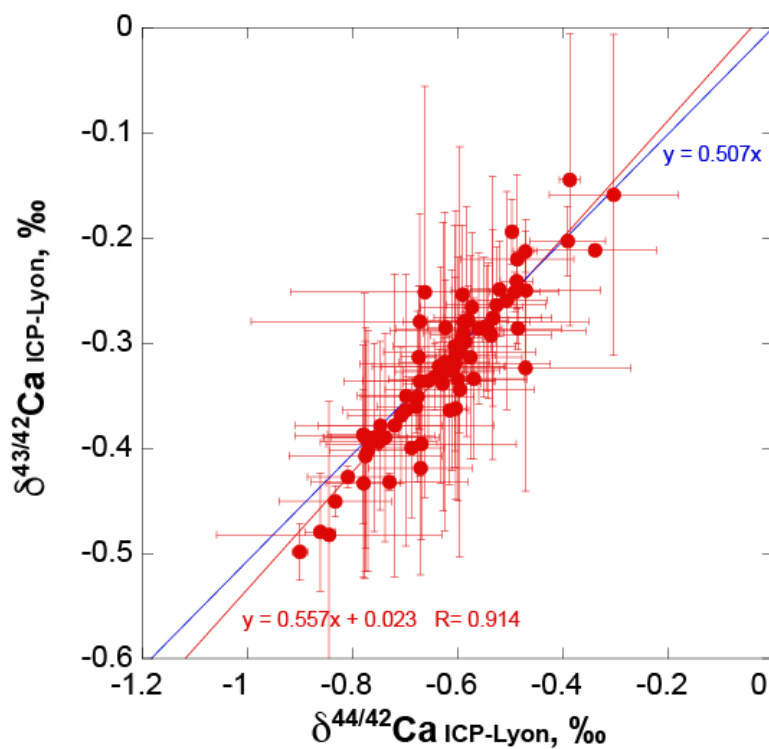


Figure S-2 Three isotopes plot: $\delta^{43/42}\text{Ca}$ values as a function of the $\delta^{44/42}\text{Ca}$ values (‰, reference standard ICP Ca-Lyon) for all samples and standards analysed in this study. Ca isotope compositions fall on a line with a y-axis intercept of 0.023 indistinguishable from theoretical 0 ‰ intercept. The slope value of this line is 0.557 (in red) very similar from the 0.507 slope (in blue) predicted by the exponential mass-dependent fractionation law.

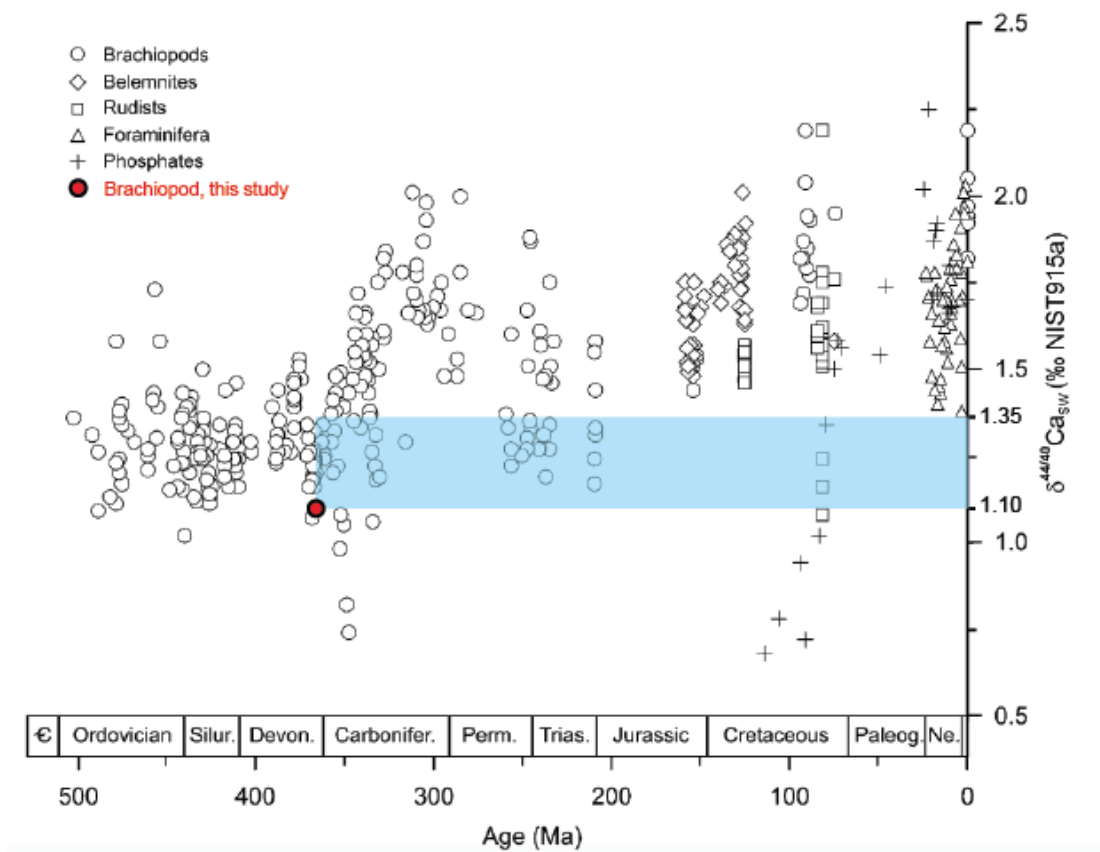


Figure S-3 Value of the $\delta^{44/40}\text{Ca}$ of seawater reconstructed from the brachiopod analysed in this study (in red) in the context of the Phanerozoic variations published by Farkaš *et al.* (2007).



Supplementary Information References

- Becker, R.T., Gradstein F.M., Hammer O. (2012) The Devonian Period. In: F.M. Gradstein, J.G. Ogg, M.D. Schmitz and G. M. Ogg. (Eds.) *The Geologic Time Scale 2012* Oxford, Elsevier. Volume 2, 559-602.
- Brazier, J.-M., Suan, G., Tacail, T., Simon, L., Mattioli, E., Martin, J.E., Balter, V. (2015) Calcium isotope evidence for dramatic increase of continental weathering during the Toarcian Oceanic Anoxic Event (Early Jurassic). *Earth and Planetary Science Letters* 411, 164-176.
- Farkaš, J., Böhm, F., Wallmann, K., Blenkinsop, J., Eisenhauer, A., van Geldern, R., Munnecke, A., Voigt, S., Veizer, J. (2007) Calcium isotope record of Phanerozoic oceans: implications for chemical evolution of seawater and its causative mechanisms. *Geochimica Cosmochimica Acta* 71, 5117-5134.
- Feist, R., Becker, R.T. (1997) Discovery of Famennian trilobites in Australia (Late Devonian, Canning Basin, NW Australia). *Geobios* 20, 231-242.
- Flajs, G., Feist, R. (1988) Index conodonts, trilobites and environment of the Devonian/Carboniferous boundary beds at La Serre (Montagne Noire, France). Devonian-Carboniferous boundary – Results of recent studies. *Courier Forschungsinstitut Senckenberg* 100, 53-107.
- Girard, C., Feist, R. (1997) Eustatic trends in conodont diversity across the Frasnian/Famennian boundary in the stratotype area, Montagne Noire, France. *Lethaia* 29, 329-337.
- Girard, C., Klapper, G., Feist, R. (2005) Subdivision of the terminal Frasnian linguiformis conodont Zone, revision of the correlative interval of Montagne Noire Zone 13, and discussion of stratigraphically significant associated trilobites. In: Over, D.J., Morrow, J.R., Wignall, P.B. (Eds.) *Understanding Late Devonian and Permian-Triassic Biotic and Climatic Events: Towards an integrated approach*. Developments in Palaeontology and Stratigraphy Series, pp. 181-198.
- Girard, C., Phuong, T.H., Savage, N.M., Renaud S. (2010) Temporal dynamics of the geographic differentiation of Late Devonian *Palmatolepis* assemblages in the Prototethys. *Acta Palaeontologica Polonica* 55, 675-687.
- Girard, C., Cornée, J.-J., Corradini, C., Fravallo, A., Feist, R. (2014) Palaeoenvironmental changes at Col des Tribes (Montagne Noire, France), a reference section for the Famennian of north Gondwana-related areas. *Geological Magazine* 151, 864-884.
- Joachimski, M.M., Buggisch, W., (1993) Anoxic events in the late Frasnian-Causes of the Frasnian-Famennian faunal crisis?. *Geology*, 21, 675-678.
- Heuser, A., Eisenhauer, A. (2008) The Calcium Isotope Composition ($\delta^{44/40}\text{Ca}$) of NIST SRM 915b and NIST SRM 1486. *Geostandards Geoanalytical Research* 32, 311-315.
- Heuser, A., Tütken, T., Gussone, N., Galer, S.J.G. (2011) Calcium isotopes in fossil bones and teeth – Diagenetic versus biogenic origin. *Geochimica et Cosmochimica Acta* 75, 3419-3433.
- Lazreq, N. (1999) Biostratigraphie des conodontes du Givétien au Famennien du Maroc central - Biofaciès et événement Kellwasser. *Courier Forschungsinstitut Senckenberg* 214, 1-111.
- Le Houedec, S., Girard, C., Balter, V. (2013) Conodont Sr/Ca and $\delta^{18}\text{O}$ record seawater changes at the Frasnian-Famennian boundary. *Palaeogeography, Palaeoclimatology, Palaeoecology* 376, 114-121.
- Martin, J. E., Tacail, T., Adnet, S., Girard, C., Balter, V. (2015) Calcium isotopes reveal the trophic position of extant and fossil elasmobranchs: *Chemical Geology* 415, 118-125.
- Martin, J. E., Tacail, T., and Balter, V. (2017) Non-traditional isotope perspectives in vertebrate palaeobiology. *Palaeontology* 60, 485-502.
- Phuong, T.H. (1998) Upper Devonian Conodont Biostratigraphy in Viêt Nam. *Journal of Geology Series B*, 11-12, 76-84.
- Pruss, S.B., Blättler, C.L., Macdonald, F.A., Higgins, J.A. (2018) Calcium isotope evidence that the earliest metazoan biomineralizers formed aragonite shells. *Geology* 46, 763-766.
- Reynard, B., Balter, V. (2014) Trace elements and their isotopes in bones and teeth: diet, environments, diagenesis, and dating of archeological and paleontological samples. *Palaeogeography, Palaeoclimatology, Palaeoecology* 416, 4-16.
- Tacail, T., Albalat, E., Télouk, P., Balter, V. (2014) A simplified protocol for the measurement of Ca isotopes in biological samples. *Journal of Analytical Atomic Spectrometry* 29, 529-535.

